ESJ Natural/Life/Medical Sciences Peer-reviewed

Energy Recovery from *Ulva* sp. Algal Biomass in the Form of Fuel Briquettes: The Influence of the Binder on Energy and Mechanical Performance

Kalidou Ba
Mamadou Faye
Alpha Ousmane Toure
Water, Energy, Environment and Industrial Processes Laboratory (LE3PI),
Ecole Supérieure Polytechnique (ESP), Dakar-Fann, Senegal
Cheikh Anta Diop University of Dakar, Dakar-Fann, Senegal

Doi:10.19044/esj.2026.v22n24p33

Submitted: 23 March 2026
Accepted: 12 August 2026
Published: 31 August 2026

Copyright 2026 Author(s)
Under Creative Commons CC-BY 4.0
OPEN ACCESS

Cite As:
Ba, K., Faye, M., & Toure, A.O. (2026). *Energy Recovery from Ulva sp. Algal Biomass in the Form of Fuel Briquettes: The Influence of the Binder on Energy and Mechanical Performance.* European Scientific Journal, ESJ, 22 (24), 33.
https://doi.org/10.19044/esj.2026.v22n24p33

Abstract

The use of algae for energy production in the form of fuel briquettes represents a promising approach to reducing greenhouse gas emissions and promoting the energy transition. These briquettes offer a sustainable and renewable alternative to global dependence on fossil fuels. This study aims to characterise and produce fuel briquettes made from macroalgae of the genus *Ulva sp.,* collected from the jetty at SENELEC's C3 power station in Dakar (Senegal), with a view to using them as an alternative fuel to charcoal and butane gas for domestic cooking. The production method involves mixing a constant mass of dried seaweed powder with varying proportions of a mineral binder ranging from 20 % to 50 %, derived from fluosilicic acid, a by-product of the Senegalese chemical industry. Four briquette formulations were thus produced: BAL20, BAL30, BAL40 and BAL50. Physico-chemical analyses (moisture content, ash content, volatile matter and total organic carbon) and combustion tests (lower calorific value, burning time) were carried out to assess their energy performance. The results showed that the BAL20 formulation performed best, with a lower calorific value of 1,778 kcal/kg and a burn time of 85 minutes, outperforming the other formulations studied.

ISSN: 1857-7881 (Print)
e-ISSN 1857-7431 (Online)

Analysis of variance (ANOVA) indicates that ash content (ASH) has a highly significant effect on the lower calorific value ($p = 0.0307 < 5\ \%$). These results suggest that seaweed briquettes produced using industrial waste as a binder represent a viable and environmentally friendly energy alternative that can contribute both to the management of coastal seaweed biomass and to the energy transition in Senegal.

Keywords: *Ulva* sp.; fuel briquettes; energy recovery; calcium silicate; calorific value

1. Introduction

The use of current energy sources such as fossil fuels poses a genuine environmental problem, particularly in terms of air and water pollution in recent years (François et al., 2025; Sundaram et al., 2025). These negative consequences have spurred interest in developing new technologies to generate clean energy, primarily through the utilisation of surplus plant and animal waste (Nzihou et al., 2024; Rath et al., 2024). According to recent statistics from the Food and Agriculture Organisation of the United Nations (FAO), global seaweed production has continued to rise. Around 30.1 million tonnes of aquatic plants (mainly seaweed, worth 11.7 billion US dollars) were produced in 2016, more than double the figure recorded in 2000 (FAO, 2024)). Seaweed is regarded as an important source of biomass for energy production due to its rapid growth and photosynthetic efficiency; however, its use for energy recovery remains limited on a global scale (Baghel et al., 2020; Yaman & Kucukbayrak, 2013) . Current uses of aquatic biomass mainly involve the production of cosmetics, fertilisers, industrial gums (phytocolloids), chemicals and foodstuffs, particularly in Asia (Jabeen et al., 2025; C. Li et al., 2024). The technical feasibility of converting marine microalgae into a renewable energy source has been investigated by several researchers. Wal et al. (2013) demonstrated the potential to produce butanol via fermentation and biogas via anaerobic digestion. With regard to macroalgae, anaerobic digestion has been studied for biogas production (Akila et al., 2019), pyrolysis for bio-oil production (Amrullah et al., 2022) and fermentation for bioethanol production (Toro-Mellado et al., 2025). Furthermore, Kim et al. (2019) and Yaman & Kucukbayrak (2013) demonstrated the co-production of alginate and biodiesel from the brown seaweed Laminaria japonica, via the heterotrophic cultivation of an oil-producing yeast in the supernatant of an autoclaved seaweed solution, prior to the solid-phase extraction of alginate. These processes present major constraints in resource-limited contexts, notably high capital costs, the need for specialised infrastructure and difficulties in scaling up. However, the briquetting technique is a simple, low-cost and accessible technology that

ISSN: 1857-7881 (Print)
e-ISSN 1857-7431 (Online)

requires neither complex equipment nor expensive chemical inputs. It therefore offers a relevant application for the valorisation of local algal biomass, which is available in large quantities along the Senegalese coastline. Among the macroalgae found in Senegal are green algae of the genus Ulva sp., which are considered one of the most promising sources of biomass (Amrullah et al., 2022). They are relatively low in carbon but often rich in nitrogen, phosphorus and other nutrients compared with many types of terrestrial biomass (Sheppard et al., 2023). Approximately 3,852,000 kg *of* fresh *Ulva sp*. is harvested per season (March to August). This represents a potential energy source facing a challenge in terms of utilisation. Their presence is partly due to the discharge of waste or untreated sewage into the sea, which causes them to proliferate. Once collected, exposure to sunlight accelerates the decomposition process, producing hydrogen sulphide, ammonia and methane (Ahmed et al., 2024). At certain concentrations, these gases can be highly dangerous to humans and animals (Jo et al., 2013; Lars Ole et al., 2023) . To date, no study has been carried out on the utilisation of Ulva sp. green algae sourced from the cooling water of the condensers at the Cap des Biches power station in Dakar.

With this in mind, this study aims to propose the utilisation of Ulva sp. biomass in the form of fuel briquettes, using calcium silicate as a binder synthesised from fluosilicic acid, a by-product of the Senegalese chemical industry. This approach will enable algal waste to be converted into domestic energy and a local industrial by-product to be utilised as a mineral binder. The objective is to assess the influence of the binder content (20–50 per cent) on the physico-chemical, energy and mechanical properties of the briquettes produced, in order to identify the optimal formulation suited to domestic firing conditions in Senegal.

2. Materials and Methods

2.1. Raw material

A 50 kg mass of *Ulva sp*. is collected between June and October at the jetty of the C3 power station – SENELEC (Cap des Biches, Dakar; 14°43'N, 17°18'W), after being retained by the Baudrey filters in the cooling circuit. It is then transported to the laboratory to be dried out of direct sunlight at room temperature for at least 24 hours, spread out on a flat surface to ensure better aeration. This step is important for determining the water content of the fresh seaweed. The second stage involves drying the seaweed in an oven at a temperature of approximately 105°C for 24 hours. Following this stage, it is ground using a metal pestle and mortar, then sieved through a 300 µm mesh sieve. The Ulva species used are shown in Figure 1.

ISSN: 1857-7881 (Print)
e-ISSN 1857-7431 (Online)



Figure 1: *Ulva* sp., near the Cap des Biches channel

2.2. Synthesis of the binder (calcium silicate)

Under normal temperature and pressure conditions, a volume of 377 mL of 25 % fluosilicic acid reacts instantaneously with a mass of 90 g of sodium chloride (NaCl). In accordance with stoichiometric proportions, this reaction produces hydrochloric acid (18 % HCl) and sodium fluorosilicate (Na_2SiF_6) (equation 1), which precipitates as a thick, gelatinous cake. The reaction took 15 minutes to complete. At the end of the reaction, vacuum filtration was carried out. The hydrochloric acid obtained is collected in a vacuum flask and the sodium fluorosilicate is retained on the filter as a cake. This precipitate is then dried at 110 °C in a MEMMERT-type oven for 24 hours. The simplified procedure for this first stage of synthesis is illustrated in Figure 2.

$$H_2SiF_6 + 2NaCL \rightarrow Na_2SiF_6 + 2HCL \quad (1)$$

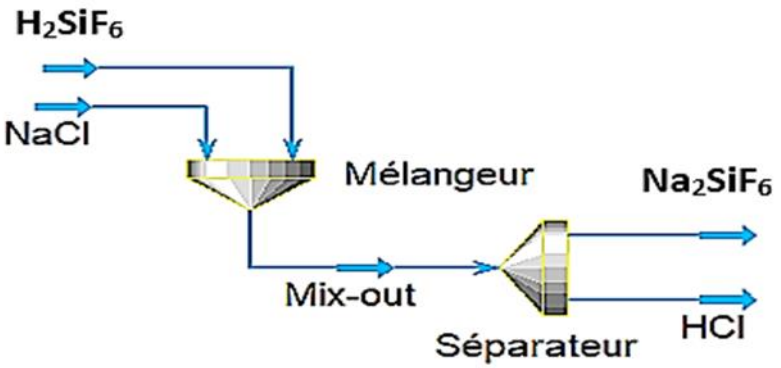


Figure 2: Process for the production of sodium fluorosilicate

ISSN: 1857-7881 (Print)
e-ISSN 1857-7431 (Online)

The sodium fluorosilicate (Na_2SiF_6) obtained in the first stage of synthesis, after being filtered, dried and ground, is causticised with slaked lime for 150 minutes at 50 °C. This process involves first mixing 100 g of sodium fluorosilicate with 600 mL of distilled water heated to 50 °C. Next, 114.15 g of slaked lime is added. At the end of the process, vacuum filtration is carried out to recover the aqueous phase, which constitutes the sodium silicate (equation 2). A simplified flowchart of the process is shown in Figure 3.

$$Na_2SiF_6 + 3Ca(OH)_2 \quad H_2O \rightarrow \quad Na_2SiO_3 + 3CaF_2 + 3H_2O \tag{2}$$

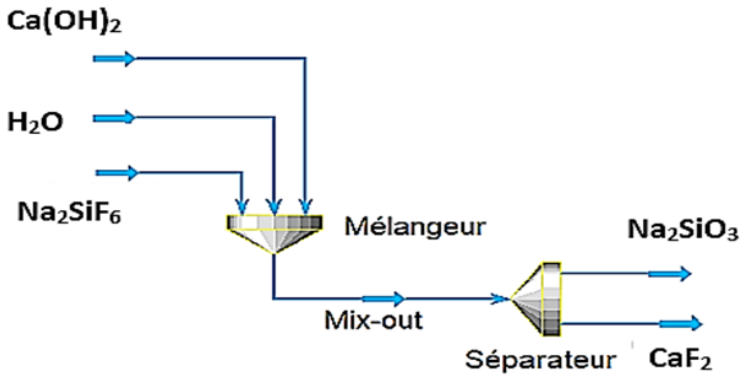


Figure 3: Process for the production of sodium silicate

The sodium silicate thus obtained is subjected to a further causticisation reaction with 43.29 g of $Ca(OH)_2$ at a temperature of 50°C for 150 minutes to produce calcium silicate and a 3 % sodium hydroxide solution (BA et al., 2022) (equation 3). Vacuum filtration is carried out to separate the solid phase from the aqueous phase. The resulting cake is dried in an oven, and the yield of calcium silicate obtained is 78.67 %. This process is illustrated in Figure 4.

$$Na_2SiO_3 + Ca(OH)_2 \rightarrow 2NaOH + CaSiO_3 \tag{3}$$

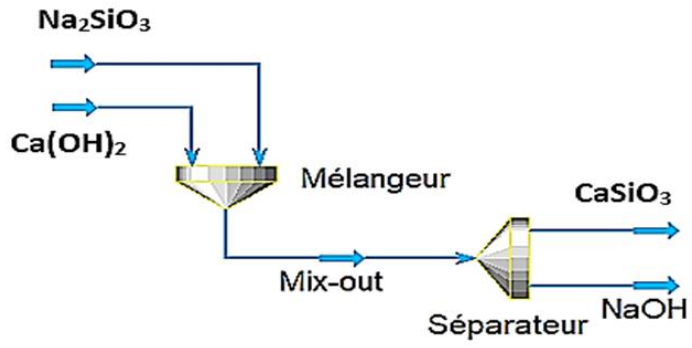


Figure 4: Process for producing calcium silicate

ISSN: 1857-7881 (Print)
e-ISSN 1857-7431 (Online)

2.3. Method for producing briquettes

The seaweed powder obtained is mixed with the mineral binder ($CaSiO_3$) and wood shavings. A constant quantity of wood shavings, amounting to approximately 20 %, was incorporated into each formulation in order to increase the density of the mixture and improve its workability, as the seaweed powder alone is too light to be extruded properly. To investigate the effect of the binder content, five types of briquettes were produced, each with a total mass of 500 g, by varying the percentage of $CaSiO_3$ from 20 to 50 %, namely BAL50 (50 per cent $CaSiO_3$), BAL40 (40 per cent $CaSiO_3$), BAL30 (30 per cent $CaSiO_3$) and BAL20 (20 per cent $CaSiO_3$). For each formulation (BAL20, BAL30, BAL40 and BAL50), a batch of briquettes was produced (up to 25 briquettes per formulation) in order to have a sufficient number of samples for all the physico-chemical analyses, drop tests and combustion tests. For each analysis, two measurements were taken on two separate briquettes from the same batch. The mixture obtained from each formulation was fed directly into a homemade extruder, comprising a 0.075 kW three-phase motor and weighing a total of 16.29 kg. A screw rotating at 280 rpm compresses the paste inside the cylinder. The briquettes emerge in a cylindrical shape thanks to a cone positioned at the extruder outlet (Figure 5). The production capacity of this machine is approximately 200 kg/h. The process flow diagram is shown in Figure 6.



Figure 5: EMIE-type extruder

ISSN: 1857-7881 (Print)
e-ISSN 1857-7431 (Online)

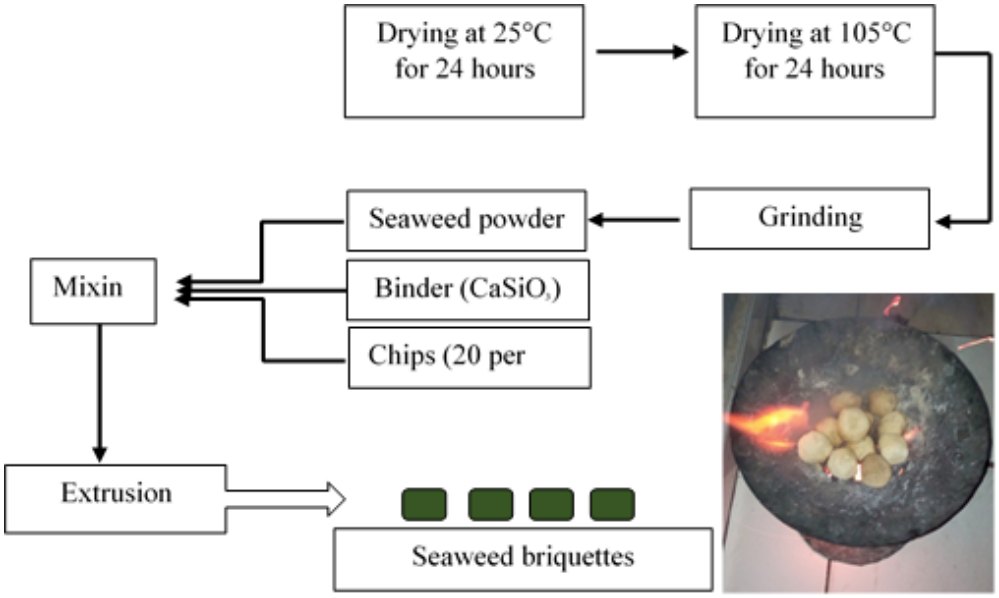


Figure 6: Process for producing briquettes made from *Ulva* sp.

2.4. Characterisation of fuel briquettes

2.4.1. Physico-chemical analyses

Following the formulation stage, the fuel briquettes are characterised by determining their moisture content, ash content and lower calorific value. These analyses were carried out by the DANGOTE Cement analysis laboratory in accordance with standard NF B55-101.

2.4.2. X-ray fluorescence (XRF) analysis

The mineral composition was determined by X-ray fluorescence spectrometry, using the Niton XL3T XRF analyser connected to a computer equipped with NDTr 6.5.2 software for data acquisition and processing. This is a rapid, non-destructive multi-element analytical technique that enables the identification and quantification of most of the chemical elements present in a sample.

For each analysis, 1.2 g of powder was mixed with 0.12 g of binder (Hoescht wax), then placed into a compression mould. A pressure of approximately 15 tonnes was applied using a press for 2 to 3 minutes to produce a compact pellet suitable for analysis. The pellets were then analysed using the Niton XL3T XRF analyser, which had been previously calibrated using certified standards.

2.4.1.2. Determination of moisture content

To determine the moisture content (H), 2 g of each briquette sample was weighed into a crucible of known mass. The crucible containing the

ISSN: 1857-7881 (Print)
e-ISSN 1857-7431 (Online)

sample was placed in a calorimetric oven at 105 °C. The crucible was removed and placed in a desiccator, then left to cool to room temperature, after which it was weighed again. This procedure was repeated until a constant mass was obtained. The moisture content was calculated using equation 4.

$$H = \frac{m_1 - m_2}{m_1} * 100 \quad (4)$$

Where:
m_1: the initial mass of the sample (g)
m_2: the final mass of the dried sample (g)

2.4.1.3. Ash content

The ash content (AC) was determined by weighing 2 grams of oven-dried briquettes in a crucible of known mass. The briquette was placed in an oven for approximately 3 hours and maintained at a constant temperature of 600 °C until ash was obtained. The ash content was calculated using equation 5.

$$AC = \frac{m_4}{m_3} * 100 \quad (5)$$

m_3: the mass of the dried sample (g)
m_4: the mass of ash (g)

2.4.1.4. Total organic carbon content

Total organic carbon (TOC) was determined using the Walkley-Black method, based on oxidation with potassium dichromate in an acidic medium, followed by titration with ferrous sulphate. The samples were ground, and a mass of between 0.1 g and 1 g was placed in an Erlenmeyer flask. This sample was mixed with 10 mL of 1 N potassium dichromate solution and 20 mL of concentrated sulphuric acid. The mixture was stirred for 1 minute and then left to stand for 30 minutes. Next, 200 mL of distilled water, 10 mL of phosphoric acid and 10 to 15 drops of the ferroin indicator solution were added. The resulting solution was titrated with 0.5 N ferrous sulphate. The percentage of carbon in the sample is determined using equation 6.

$$TOC = \frac{(A - B) * V * G * 100}{P * A} \quad (6)$$

Where V = 10 mL and G = 0.004
TOC: total organic carbon (%)
A: volume of ferrous sulphate used for the blank (mL)

ISSN: 1857-7881 (Print)
e-ISSN 1857-7431 (Online)

B: volume of ferrous sulphate used for the sample (mL)
V: volume of dichromate added initially
G: number of g of C per ml of dichromate
P: weight of the titrated sample on a dry basis (g)

2.4.1.5. Determination of the gross calorific value

The calorific value was determined using an XRY-1A type calorimetric bomb. This involves placing the sample on the sample holder inside the bomb. The ignition wire is connected to the holder and the ignition circuit, after which the bomb is sealed. Several purge cycles were carried out, followed by filling the bomb with O_2 at the specified pressure (20 - 30 bar), whilst checking for leaks. The bomb is then immersed in the calorimeter, which is filled with a known mass of water, and the stirring system is switched on. When the initial temperature (T_i) stabilises, it is recorded and the electric ignition is triggered to ensure complete combustion. After combustion, the final temperature (T_f) of the system in its steady state is recorded. The temperature change (ΔT), the net energy released by combustion (Q_{total}), the corrected net energy released (Q_{sample}), the gross calorific value (PCS) and the net calorific value (PCI) are calculated using the following equations:

$$\Delta T = T_f - T_i \tag{7}$$

$$Q_{totale} = K\Delta T \tag{8}$$

$$Q_{sample} = Q_{total} - Q_{wire} - Q_{other_{corrections}} \tag{9}$$

$$PCS = \frac{Q_{sample}}{m} \tag{10}$$

$$PCI = PCS - \left(m_{H2O} - \Delta H_{vap}\right) \tag{11}$$

Where:
K: The calorimetric constant of the system (J/°C), obtained by calibration
Q_{wire}: the energy supplied by the ignition wire, determined by testing or provided
$Q_{other_corrections}$: comprises minor thermochemical corrections relating to secondary reactions that occur in the bomb
m: is the mass of the sample (g)
m_{H2O} : mass of water formed during combustion, per kg of fuel
ΔH_{vap} : latent heat of vapourisation of water

ISSN: 1857-7881 (Print)
e-ISSN 1857-7431 (Online)

2.4.2. Mechanical test

This test involves determining the impact resistance (IR) in order to assess the behaviour of the briquettes during handling, transport and unloading. The method complies with the ASTM D440-49 standard. It involves dropping a briquette three times onto a solid surface from a height of 1.8 m. The mass of the briquette is measured before the test. The impact resistance is then calculated using equation 12.

$$IR = 100 - \frac{m_0 - m_1}{m_0} * 100 \quad (12)$$

m_0 : is the mass of the briquette measured before the drop
m_1 : is the mass of the briquette after tumbling

2.4.3. Combustion test

This analysis involves determining the combustion parameters of the briquettes, in particular the time taken for the water to boil. To do this, a saucepan containing 250 mL of water is heated on a fire fuelled by 250 g of briquettes in a sheltered, wind-free location to simulate cooking conditions. The water temperature is recorded every 5 minutes using a probe thermometer.

2.4.4. Analysis of Variance (ANOVA)

To assess the influence of ash content (ASH), total organic carbon (TOC) and moisture content (H) on the lower calorific value (PCI) of the briquettes, an analysis of variance (ANOVA) was carried out. This allows the proportion of variability explained by each factor to be compared with the residual variability of the model.

The ANOVA tests the null hypothesis (H_0) that all coefficients associated with each variable are zero, i.e. that none of the parameters considered has a significant effect on the PCI. The alternative hypothesis (H_1), on the other hand, states that at least one factor influences the PCI.

3. Results and discussion

3.1. Characterisation of Ulva species using X-ray fluorescence (XRF)

The various values obtained during elemental characterisation are set out in Table 1. The results show that Ulva sp. consists mainly of calcium (Ca: 47653.96 ppm) and potassium (K: 45509.60 ppm). Trace elements were also detected, notably magnesium (Mg: 8077.35 ppm), sulphur (S: 4977.71 ppm), phosphorus (P: 3055.05 ppm) and iron (Fe: 2,493.79 ppm). Mercury, lead and cadmium were not detected in the samples analysed, as their concentrations were below the instrument's detection limit. These results are partly comparable to those reported by Czerwik-Marcinkowska et al. (2020) on the elemental characterisation of Ulva pilifera, who identified 14 elements (Al,

ISSN: 1857-7881 (Print)
e-ISSN 1857-7431 (Online)

Ba, Br, Ca, Cl, Fe, I, K, Mg, Mn, Na, P, S and Si) in the thalli, with calcium as the dominant element, followed by sulphur, silicon and magnesium. Although calcium is also the dominant element in our study, its concentration remains lower than that reported by these authors, which could be explained by species-specific differences, distinct environmental conditions and the nature of the collection waters specific to the Cap des Biches site.

However, our results differ from those of Mouga et al. (2025), who reported sodium as the predominant element, with a concentration of 73.80 ± 0.45 mg/g in Ulva sp. collected from the open marine environment. The absence of detectable sodium in our samples could be explained by the fact that the algae originate from the cooling waters of the condensers at the Cap des Biches power station, a confined environment whose ionic composition differs significantly from that of open seawater. Furthermore, the season of collection (March to August) and possible industrial inputs from the site could also contribute to this particular mineral profile, dominated by calcium and potassium.

Table 1: Mineral composition of the *Ulva sp*.-type macroalgae

Chemical elements	Values in ppm (mg/kg)
Mo	0.112
Pb	< 0.001
Se	0.174
As	25.86
Hg	< 0.001
Zn	20.378
Cu	1.145
Ni	0.192
Co	0.402
Fe	2493.788
Mn	229.17
Cr	0.795
Ca	47653.96
K	45509.6
S	4977.71
Cd	< 0.001
Mg	8077.35
P	3055.046

3.2. Physico-chemical characterisation of Ulva

The various values for physico-chemical parameters such as moisture content, ash content, total organic carbon and lower calorific value are presented in Table 2. Each experiment was repeated twice to determine the standard deviation. These parameters enable an assessment of the extent to which the proportion of calcium silicate influences the fuel quality of the briquettes.

ISSN: 1857-7881 (Print)
e-ISSN 1857-7431 (Online)

Table 2: Physico-chemical parameters of the briquettes

Physico-chemical parameters	BAL50	BAL40	BAL30	BAL20	CHAR
Moisture content (%)	6.64±0.026	6.76±0.032	6.84±0.027	6.93±0.031	5.14±0.019
TOC (%)	15.71±0.019	20.11±0.025	21.96±0.016	24.33±0.023	20.61±0.024
Ash content (%)	49.75±0.041	47.3±0.035	44.94±0.037	39.38±0.029	17.54±0.023
PCI (kcal/kg)	1289±0.024	1338±0.029	1365±0.031	1778±0.028	2939±0.032

3.3. Ash and moisture content

Ash content represents the quantity of inorganic elements and other minerals comprising the biomass that do not burn, thus leaving residues after combustion (Imaniraguha et al., 2025). Briquettes containing 50 % binder have the highest ash content, at nearly three times that of the reference charcoal (17.54 %). The ash content of sample BAL20 is 39.38 %, the lowest among the briquettes but still significantly higher than that of charcoal. This difference is mainly due to the mineral nature of the binder, which is rich in inorganic elements that contribute directly to ash formation. Furthermore, the presence of exogenous materials such as gastropods or sand in the *Ulva sp*. biomass may also increase this content. The values obtained here are lower than those reported by Olufunke O. Oyebamiji et al., which ranged from 16.70 % (peanut shells) to 79.25 % (maize straw) (Oyebamiji et al., 2025). A study has also shown that the presence of compounds such as sodium, potassium, phosphorus and chlorine in macroalgae contributes to an increase in ash content (Bilodeau et al., 2022).

With regard to moisture content, the briquettes show values within a narrow range, between 6.64 % and 6.93 %. These values are slightly higher than those of charcoal (5.14 %) and those obtained by Georges et al. for seaweed-based briquettes (4.83 %). This higher moisture content can be attributed to the hygroscopic nature of the binder, which, when suspended in water, swells and retains a significant amount of water to form an interstitial layer (Lomunyak et al., 2024). According to Nakimuli et al., an optimal moisture content improves the density, durability and compressive strength of the briquettes (Nakato et al., 2025) . Figure 7 presents a comparison of the ash and moisture contents for the different samples.

ISSN: 1857-7881 (Print)
e-ISSN 1857-7431 (Online)

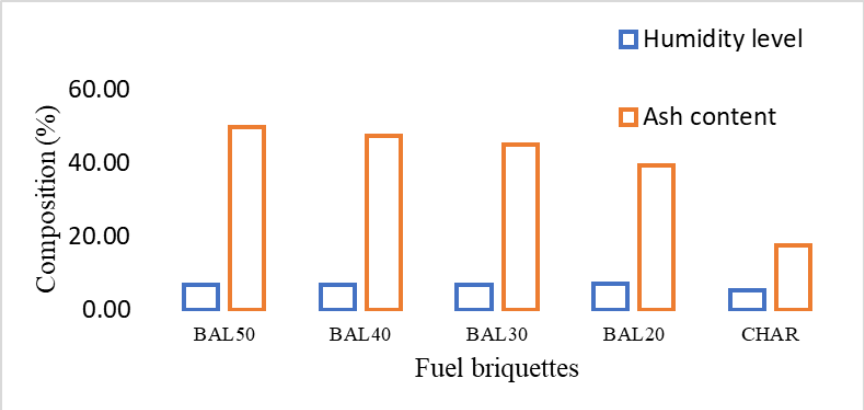


Figure 7: Effect of binder percentage on moisture content and ash content

3.4. Total organic carbon (TOC)

Total organic carbon includes all forms of organic carbon, whether dissolved, volatile or solid. It is distinct from fixed carbon, which corresponds to the fraction of carbon remaining after the removal of moisture, volatile matter and ash. Among all the samples analysed, the TOC content ranges from 15.71 % to 24.33 %. It decreases with the gradual addition of binder from 20 % to 50 %. The binder used is a mineral material; its incorporation at high levels contributes to a reduction in the organic carbon content. BAL20-type briquettes have a TOC content of 24.33 %, which is higher than that of BAL50, BAL40 and BAL30 briquettes. It has been reported in the literature that green algae biomass of *the Ulva sp.* type is very rich in organic compounds (Toro-Mellado et al., 2025) . This is why , Dogmaz and Cavas used biomass derived from *Ulva lactuca* blooms to produce biohydrogen via silver nanoparticles (Dogmaz & Cavas, 2023) . Figure 8 shows the total organic carbon content of the different briquettes.

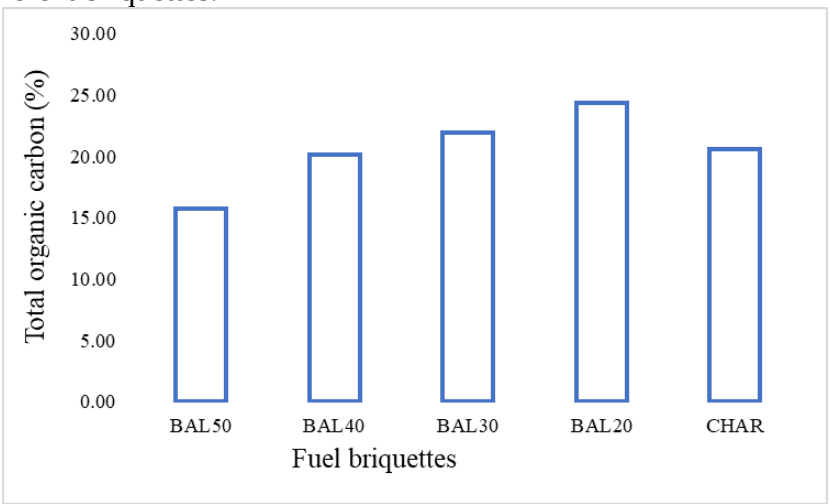


Figure 8: Effect of binder percentage on TOC

ISSN: 1857-7881 (Print)
e-ISSN 1857-7431 (Online)

3.5. Lower Calorific Value

The results obtained show that the lower calorific value (PCI) of charcoal (2939 kcal/kg) is higher than that of the fuel briquettes developed. This high value is due to the presence of lignin, the decomposition of which generates a high proportion of fixed carbon. However, the results reveal an increasing trend in the LHV as the percentage of binder decreases, from 1,289 kcal/kg for the BAL50 to 1,778 kcal/kg for the BAL20 (Table 2). These values all remain lower than that of charcoal, and only the BAL20 briquettes have the highest calorific value among the briquettes tested. This decrease in calorific value can be explained by the presence of the binder in the samples and also by the relatively low organic carbon content. Calcium silicate reduces the calorific value of the fuel briquettes due to the presence of minerals within them. The value obtained for the BAL20 briquettes is lower than that reported by Brice et al., which is 10 MJ/kg (2388.45 kcal/kg). This observed discrepancy can be explained by the fact that their briquettes were produced using wood with lignin and cellulose contents of 26.6 % and 50.4 % respectively (Martial et al., 2025). Figure 9 illustrates the gross calorific values of the various fuels.

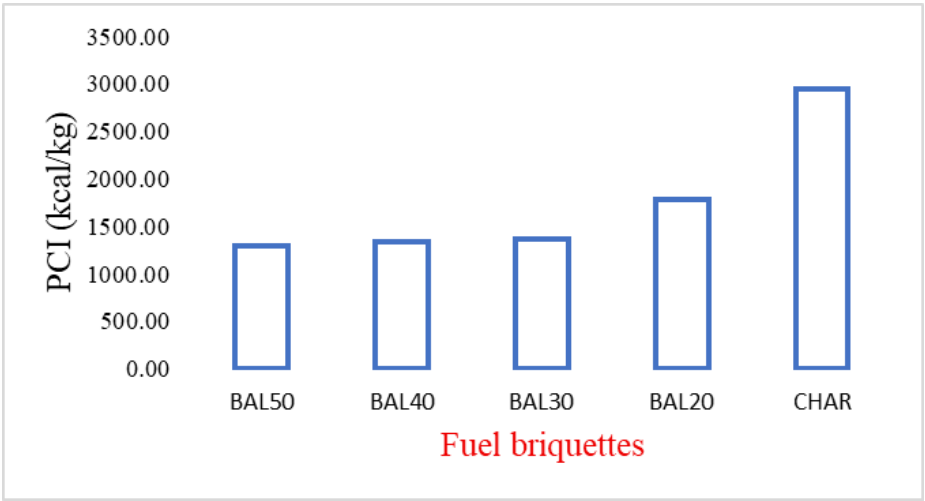


Figure 9: Effect of binder percentage on PCI

3.6. Analysis of variance (ANOVA)

The analysis of variance carried out on the lower calorific value (PCI) as a function of ash content (ASH), total organic carbon (TOC) and moisture content (H) reveals that the variability in PCI is mainly explained by the ash content. The effect of ASH is highly significant ($p = 0.0307 < 0.05$), indicating a clear and direct influence of the mineral fraction on the calorific value.

To quantify this relationship, a Pearson correlation analysis was carried out. Ash content shows the strongest negative correlation with the PCI ($r = -0.95$; $R^2 = 0.90$), confirming that ASH alone accounts for approximately

ISSN: 1857-7881 (Print)
e-ISSN 1857-7431 (Online)

90% of the observed variance in the PCI. Each 1 per cent increase in ash content is associated with a decrease of approximately 48 kcal/kg in the calorific value. This relationship is explained by the inorganic nature of the $CaSiO_3$ binder, which does not contribute to combustion and dilutes the energy content of the briquettes. By contrast, moisture content ($p = 0.4547$) and total organic carbon ($p = 0.4432$) did not show any statistically significant effects at the $\alpha = 0.05$ threshold, suggesting that, within the range of variation studied, these parameters do not exert a detectable influence on the PCI.

Biomass briquettes intended for domestic use are classified as having an ash content of less than 4 per cent, a moisture content of less than 13 per cent and a minimum net calorific value of 14.5 MJ/kg (Walozi et al., 2026). The formulations studied, with ash contents ranging from 39.38 % (BAL20) to 49.75 % (BAL50), far exceed this threshold. This high ash content affects combustion efficiency by reducing the fuel's energy density, promoting clogging and slag formation, and inhibiting complete combustion (Walozi et al., 2026). However, for the traditional open hearths commonly used in sub-Saharan Africa, this constraint is less limiting, and the obtained PCI) values (1289 to 1778 kcal/kg) remain suitable for domestic use in this context. Similar results were reported by Huihui Liu et al. in their study of the hydrothermal carbonisation of natural microalgae with high ash content, where a negative correlation between the mineral fraction and calorific value was observed (Liu et al., 2019). The individual effects of ASH, TOC and H on the gross calorific value are illustrated in Figure 10.

ISSN: 1857-7881 (Print)
e-ISSN 1857-7431 (Online)

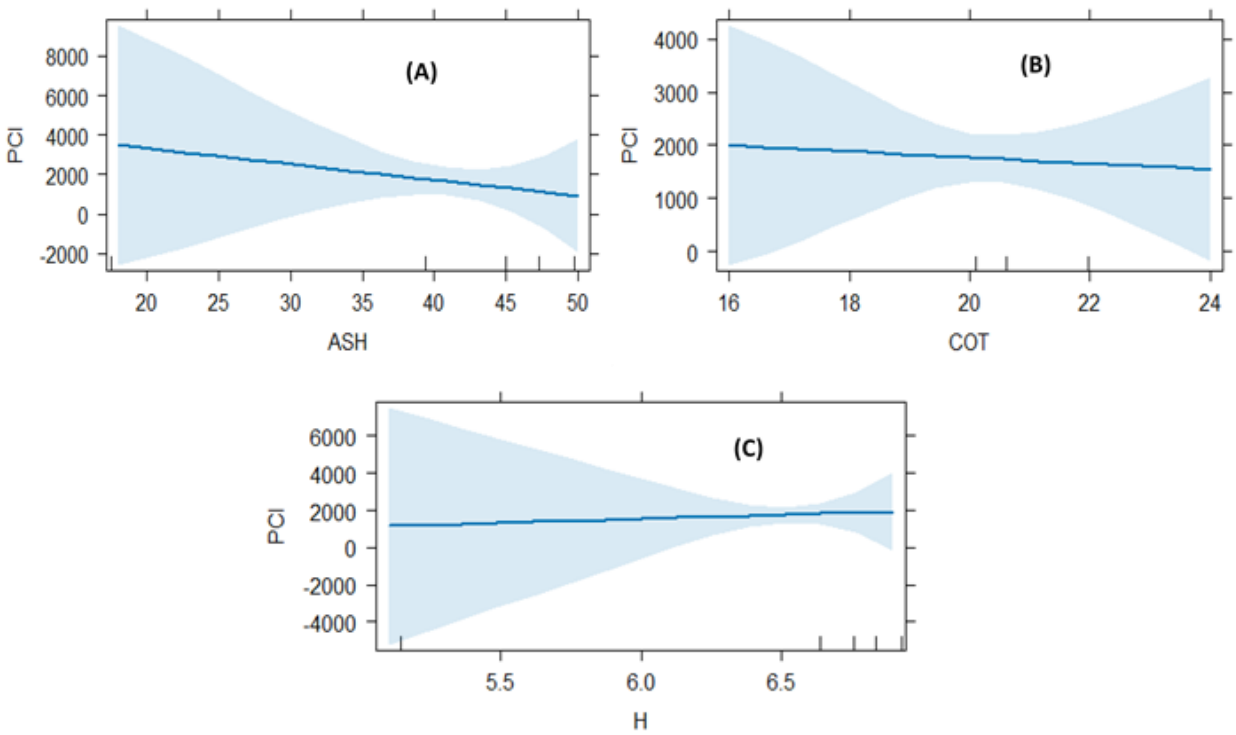


Figure 10: Effects of ash content (A), total organic carbon (B) and moisture content (C) on the lower calorific value

3.7. Impact resistance

Impact resistance ranges from 79 % (BAL20) to 84 % (BAL50) (Table 3), following a trend directly proportional to the binder content: the higher the calcium silicate content, the greater the mechanical durability. This result highlights a fundamental trade-off between mechanical properties and energy performance, directly linked to the role of calcium silicate as a structuring binder. According to Mitchual et al. (2013), briquettes with an impact resistance greater than 80 % are considered to be highly durable; in this respect, the BAL30, BAL40 and BAL50 formulations meet this criterion. These values are comparable to those reported by Njoka et al. (2024), who obtained an average impact resistance of 95.2 % for charcoal briquettes using seaweed as a binder, produced under similar conditions of manual manufacture. Nonsawang et al. (2024) also confirmed that impact resistance increases with binder content, which is consistent with the trends observed in the present study.

ISSN: 1857-7881 (Print)
e-ISSN 1857-7431 (Online)

Table 3: Effect of the percentage of calcium silicate on impact resistance

Briquettes	BAL20	BAL30	BAL40	BAL50
Mechanical durability (%)	79	81	82	84

3.8. Combustion test

Figure 11 shows the change in water temperature, measured every 5 minutes during heating using the different types of briquettes. The results show that BAL20 is the only formulation to reach boiling point (~100°C) at 25 minutes, confirming its thermal superiority, consistent with its highest gross calorific value (1778 kcal/kg = 7.44 MJ/kg). For BAL30, a gradual rise in temperature is observed up to 84.7°C at around 25 minutes, followed by a relatively stable thermal plateau. The BAL40 and BAL50 briquettes reached their respective peaks at 69.6°C after 25 minutes and 77.6°C after 30 minutes, with less efficient combustion. This poor combustion of the BAL40 and BAL50 briquettes is probably due to the presence of very high ash content, moisture and volatile organic matter. According to Gang Li et al., several factors can affect the combustion rate; in their study, it was assumed that the higher ash content (54.3 ± 0.9 %) of the fuel was the main reason for the lower combustion rate (G. Li et al., 2022). Another study on sawdust briquettes showed that energy efficiency decreased as moisture content increased, which can reduce the combustion rate (Mkini & Bakari, 2018).

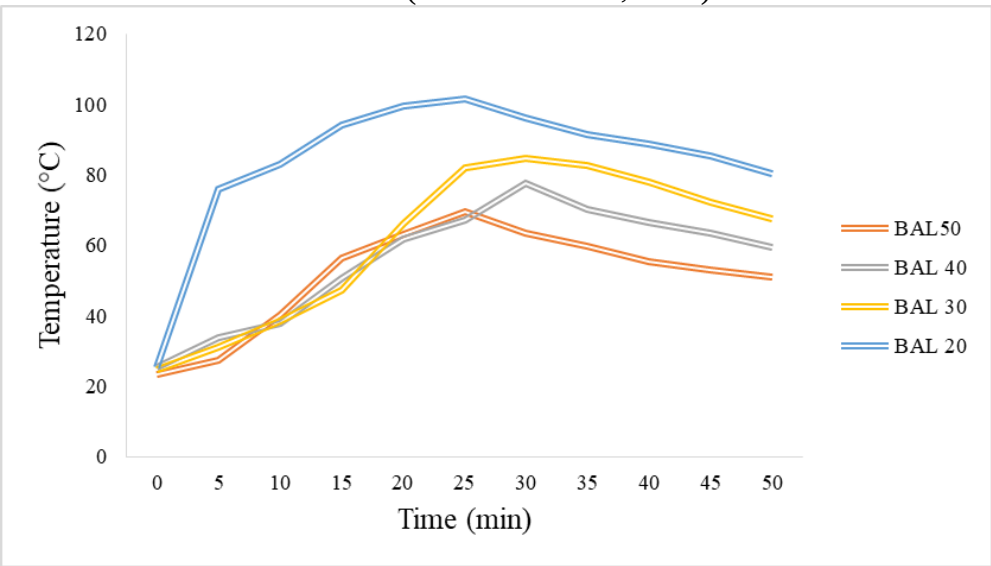


Figure 11: Change in the boiling point of water over time

Conclusion

This study has demonstrated the technical feasibility of utilising Ulva sp. waste from SENELEC's C3 power station by producing fuel briquettes as a partial substitute for conventional charcoal in the Senegalese context. The

ISSN: 1857-7881 (Print)
e-ISSN 1857-7431 (Online)

results showed that the calcium silicate content significantly influences the thermal and mechanical properties of the briquettes produced. Among the formulations tested, the BAL20 briquettes performed well, with a lower calorific value (PCI) of 1,778 kcal/kg (7.44 MJ/kg), although this value remains lower than that of conventional charcoal (PCI = 2939 kcal/kg; 12.30 MJ/kg).

Although this lower calorific value is lower than that of conventional charcoal, it remains comparable to that of other biomass briquettes reported in the literature (Mitchual et al., 2013; Njoka et al., 2024), suggesting a viable solution for domestic applications in rural areas where conventional charcoal is economically unaffordable.

Statistical analysis (ANOVA) confirmed that ash content is the most influential factor, with a statistically significant effect ($p < 0.05$; $p = 0.031$), whilst moisture content and total organic carbon (TOC) did not reach the significance threshold. This result can be explained by the small variation in moisture content between the formulations, which may have limited its discriminatory power, whilst the effect of TOT was probably masked by the dominant effect of the high content of the mineral binder. Furthermore, the mechanical strength of the briquettes increases with the proportion of binder, reaching an optimal durability of 84 % for the BAL50 briquettes.

However, the high ash content of the briquettes, particularly for the BAL20 (39.38 %), presents a major challenge for large-scale deployment in terms of the maintenance of combustion systems and the management of residues. Consequently, further studies are required to reduce the proportion of mineral binder by combining it with organic binders, in order to lower the ash content whilst preserving the mechanical integrity of the briquettes. Furthermore, a cost-benefit analysis should be carried out to assess the economic and environmental viability of the seaweed-based briquette production process.

Despite these limitations, this study represents an initial investigation into the energy recovery of Ulva sp. macroalgae, sourced from industrial cooling water, in the form of fuel briquettes, using a mineral binder derived from a by-product of the Senegalese chemical industry, subject to further optimisation of the formulation.

Conflict of Interest: The authors reported no conflict of interest.

Data Availability: All data are included in the content of the paper.

Funding Statement: The authors did not obtain any funding for this research.

ISSN: 1857-7881 (Print)
e-ISSN 1857-7431 (Online)

References:

1. Ahmed, M. S., Lebrini, M., Pellé, J., Rioual, S., Amintas, O., Boulanger, C., Lescop, B., & Roos, C. (2024). Study of atmospheric corrosion of zinc in a tropical marine environment rich in H_2S, resulting from the decomposition of *Sargassum* algae. *Materials and Corrosion*, *75*(9), 1133–1141. https://doi.org/10.1002/MACO.202414292
2. Akam, N. G., Diboma, B. S., Mfomo, J. Z., Ndiwe, B., Bôt, B. V., & Biwolé, A. B. (2024). Physicochemical characterisation of briquette fuel produced from cocoa pod husks: The case of Cameroon. *Energy Reports*, *11*, 1580–1589. https://doi.org/10.1016/j.egyr.2024.01.029
3. Akila, V., Manikandan, A., Sahaya Sukeetha, D., Balakrishnan, S., Ayyasamy, P. M., & Rajakumar, S. (2019). Biogas and biofertiliser production from marine macroalgae: An effective anaerobic digestion of *Ulva* sp. *Biocatalysis and Agricultural Biotechnology*, *18*, 101035. https://doi.org/10.1016/j.bcab.2019.101035
4. Amrullah, A., Farobie, O., Bayu, A., Syaftika, N., Hartulistiyoso, E., Moheimani, N. R., Karnjanakom, S., & Matsumura, Y. (2022). Slow pyrolysis of *Ulva lactuca* (Chlorophyta) for sustainable production of bio-oil and biochar. *Sustainability*, *14*(6), 3233. https://doi.org/10.3390/su14063233
5. BA, K., Diop, E. H. M., Toure, A. O., & Sambe, F. M. (2022). Optimisation of crystal violet adsorption by calcium silicate waste material. *Scientific African*, *18*, e01417. https://doi.org/10.1016/j.sciaf.2022.e01417
6. Baghel, R. S., Suthar, P., Gajaria, T. K., Bhattacharya, S., Anil, A., & Reddy, C. R. K. (2020). Seaweed biorefinery: A sustainable process for valorising the biomass of brown seaweed. *Journal of Cleaner Production*, *263*, 121359. https://doi.org/10.1016/j.jclepro.2020.121359
7. Bilodeau, M., Barnabé, S., Riverin, L., & Fequet, K. (2022). The potential for integrating marine algae from the Lower North Shore into Quebec's energy mix. *Revue des sciences de l'eau*, 43–47.
8. Czerwik-Marcinkowska, J., Piwowarczyk, R., Uher, B., Tomal, E., & Wojciechowska, A. (2020). X-ray fluorescence techniques in determining the habitat preferences of *species—Ulva pilifera* (Ulvales, Chlorophyta): a case study from Montenegro. *Molecules*, *25*(21), 5022. https://doi.org/10.3390/molecules25215022
9. Dogmaz, S., & Cavas, L. (2023). Biohydrogen production via green silver nanoparticles synthesised from *Ulva lactuca* bloom biomass. *Bioresource Technology*, *379*, 129028. https://doi.org/10.1016/j.biortech.2023.129028

ISSN: 1857-7881 (Print)
e-ISSN 1857-7431 (Online)

10. Farobie, O., Amrullah, A., Bayu, A., Syaftika, N., Anis, L. A., & Hartulistiyoso, E. (2022). In-depth study of bio-oil and biochar production from the macroalgae *Sargassum* sp. via slow pyrolysis. *RSC Advances*, *12*(16), 9567–9578. https://doi.org/10.1039/D2RA00702A
11. François, M., Lin, K., Hussain, J., & Mdlovu, N. V. (2025). Enhancement of biomass energy: Thermal conversion, biogas yield, and machine learning insights. *Journal of the Energy Institute*, *121*, 102131. https://doi.org/10.1016/j.joei.2025.102131
12. Goffeng, L. O., Austigard, Å. D., Svendsen, K. H., Skare, Ø., Einarsdottir, E., Madsø, L., & Heldal, K. K. (2023). A cross-sectional study of sensory-motor neuropsychological function among sewage plant and sewage network workers exposed to hydrogen sulphide whilst handling wastewater. *Annals of Work Exposures and Health*, *67*(9), 1027–1042. https://doi.org/10.1093/annweh/wxad051
13. Imaniraguha, J., Mushimiyimana, T., Lucas, C., & Condo, A. (2025). Production and characterisation of briquettes from *Panicum maximum* Jacq. (Guinea grass) and cassava peel waste. *Energy Reports*, *14*, 1043–1050. https://doi.org/10.1016/j.egyr.2025.07.033
14. Jabeen, F., Zil-E-Aimen, N., Ahmad, R., Mir, S., Awwad, N. S., & Ibrahium, H. A. (2025). Carrageenan: Structure, properties and applications with special emphasis on food science. *RSC Advances*, *15*(27), 22035–22062. https://doi.org/10.1039/d5ra03296b
15. Jo, J. Y., Kwon, Y. S., Lee, J. W., Park, J. S., Rho, B. H., & Choi, W. I. (2013). Acute respiratory distress due to methane inhalation. *Tuberculosis and Respiratory Diseases*, *74*(3), 120–123. https://doi.org/10.4046/trd.2013.74.3.120
16. Kim, G., Hwan, Y., Kim, I., & Han, J. (2019). Co-production of biodiesel and alginate from *Laminaria japonica*. *Science of the Total Environment*, *673*, 750–755. https://doi.org/10.1016/j.scitotenv.2019.04.049
17. Li, C., Liang, Y., Miao, Q., Ji, X., Duan, P., & Quan, D. (2024). The influence of microalgae fertiliser on soil water conservation and soil improvement: Yield and quality of potted tomatoes. *Agronomy*, *14*(9), 2102. https://doi.org/10.3390/agronomy14092102
18. Li, G., Hao, Y., Yang, T., Wu, J., Xu, F., Li, L., Wang, B., Li, M., Zhao, N., Wang, N., Liu, C., Huang, Z., Zhou, Y., & Zhao, Y. (2022). Air pollutant emissions from sludge-bituminous briquettes as a potential household energy source. *Case Studies in Thermal Engineering*, *37*, 102251. https://doi.org/10.1016/j.csite.2022.102251
19. Liu, H., Chen, Y., Yang, H., Gentili, F. G., Söderlind, U., Wang, X., Zhang, W., & Chen, H. (2019). Hydrothermal carbonisation of natural

ISSN: 1857-7881 (Print)
e-ISSN 1857-7431 (Online)

microalgae with a high ash content. *Fuel*, *249*, 441–448. https://doi.org/10.1016/j.fuel.2019.03.004

20. Lomunyak, G., Osodo, B., Njoka, F., & Kombe, E. (2024). Characterisation, optimisation and emission analysis of hand-made charcoal dust briquettes using starch, paper and algae binders. *Heliyon*, *10*(24), e40991. https://doi.org/10.1016/j.heliyon.2024.e40991
21. Martial, B., Lemaire, R., & Nikiema, J. (2025). Insight into the production factors influencing the physicochemical properties of densified briquettes comprising wood shavings and rice husk. *Industrial Crops and Products*, *223*, 120134. https://doi.org/10.1016/j.indcrop.2024.120134
22. Mitchual, S. J., Frimpong-Mensah, K., & Darkwa, N. A. (2013). Effect of species, particle size and compacting pressure on relaxed density and compressive strength of fuel briquettes. *International Journal of Energy and Environmental Engineering*, *4*(1), 30. https://doi.org/10.1186/2251-6832-4-30
23. Mkini, R. I., & Bakari, Z. (2018). Effect of moisture content on combustion and friability characteristics of biomass waste briquettes made by small-scale producers in Tanzania. *International Journal of Engineering Research and Reviews*, *3*(1), 66–72.
24. Mouga, T., Almeida, M. M., Pitacas, F. I., Rodrigues, A. M., Vitória, C., & Anjos, O. (2025). Elemental and nutritional characterisation using vibrational spectroscopy analysis of *Ulva* sp., *Gracilaria multipartita*, and *Sargassum muticum*. *Applied Sciences*, *15*(8), 4212. https://doi.org/10.3390/app15084212
25. Nakato, C., Kaggwa, F., De Greef, J., Kilama, D., Blondeau, J., & Kawuma, S. (2025). Review of machine learning applications for predicting the quality of biomass briquettes for sustainable and low-carbon energy solutions. *Green Energy and Resources*, *3*(3), 100130. https://doi.org/10.1016/j.gerr.2025.100130
26. Nonsawang, S., Juntahum, S., Sanchumpu, P., Suaili, W., Senawong, K., & Laloon, K. (2024). Unlocking renewable fuel: Charcoal briquette production from agro-industrial waste using cassava-based industrial binders. *Energy Reports*, *12*, 4966–4982. https://doi.org/10.1016/j.egyr.2024.10.053
27. Nzihou, A., Ifunanya, G., & Gonz, M. (2024). A review on biochar briquetting: Common practices and recommendations to enhance mechanical properties and environmental performance. *Journal of Cleaner Production*, *469*, 143193. https://doi.org/10.1016/j.jclepro.2024.143193
28. Njoka, F., Kombe, E., et al. (2024). Characterisation, optimisation and emission analysis of manually-made charcoal dust briquettes with

ISSN: 1857-7881 (Print)
e-ISSN 1857-7431 (Online)

starch, paper and algae binders. Heliyon, 10(24), e40991. https://doi.org/10.1016/j.heliyon.2024.e40991

29. Oyebamiji, O. O., Olaleru, A. S., Oyeleke, R. B., & Ofodile, L. N. (2025). Evaluation and characterisation of biochar and briquettes from agricultural waste for sustainable energy production. *Waste Management Bulletin*, *3*(3), 100198. https://doi.org/10.1016/j.wmb.2025.100198
30. Rath, D. P., Mahapatro, A., & Pattanayak, B. (2024). Briquette production and performance evaluation from coal and agricultural waste. *Materials Today: Proceedings*. https://doi.org/10.1016/j.matpr.2023.12.019
31. Sheppard, E. J., Hurd, C. L., Britton, D. D., Reed, D. C., & Bach, L. T. (2023). Seaweed biogeochemistry: Global assessment of C:N and C:P ratios and implications for ocean afforestation. *Journal of Phycology*, *59*(4), 879–892. https://doi.org/10.1111/jpy.13381
32. Sundaram, T., Kamalesh, R., Saravanan, A., Yaashikaa, P. R., Vickram, A. S., Teena, R. A., & Thiruvengadam, S. (2025). Harnessing algal biomass for renewable energy and biofuel production: Current strategies and future insights. *International Journal of Biological Macromolecules*, *319*, 145487. https://doi.org/10.1016/j.ijbiomac.2025.145487
33. Sundblad, B.-M., Larsson, B.-M., Acevedo, F., Ernstgård, L., Johanson, G., Larsson, K., & Palmberg, L. (2004). Acute respiratory effects of exposure to ammonia on healthy persons. *Scandinavian Journal of Work, Environment & Health*, *30*(4), 313–321. https://doi.org/10.5271/sjweh.800
34. Toro-Mellado, F., Piña, F., Baltrusch, K. L., Inoubli, S., Flórez-Fernández, N., Torres, M. D., Contreras-Porcia, L., & Domínguez, H. (2025). Potential applications of *Ulva* spp. *Food Bioscience*, *71*, 107256. https://doi.org/10.1016/j.fbio.2025.107256
35. Van der Wal, H., Sperber, B. L. H. M., Houweling-Tan, B., Bakker, R. R. C., Brandenburg, W., & López-Contreras, A. M. (2013). Production of acetone, butanol, and ethanol from biomass of the green seaweed *Ulva lactuca*. *Bioresource Technology*, *128*, 431–437. https://doi.org/10.1016/j.biortech.2012.10.094
36. Walozi, R., Onep, G. S., Sanusi, Y. S., Babiker, O. E., Dennison, M. S., Candia, A., & Okurut, S. (2026). *A comprehensive review of chemical treatments for biomass feedstock to enhance briquette characteristics*.
37. Yaman, S., & Kucukbayrak, S. (2013). Production of biobriquettes from carbonised brown seaweed. *Fuel Processing Technology*, *106*, 33–40. https://doi.org/10.1016/j.fuproc.2012.06.014